
Design work of the ERL-FEL as the high intense EUV light source

Norio Nakamura

High Energy Accelerator Research Organization(KEK)

ERL2015, Stony Brook, NY, USA, June 7-12, 2015.

ERL-EUV Design Group



(KEK) H. Kawata, Y. Kobayashi, T. Furuya, K. Haga,
I. Hanyu, K. Harada, T. Honda, Y. Honda, E. Kako,
Y. Kamiya, R. Kato, S. Michizono, T. Miyajima, H. Nakai,
N. Nakamura, T. Obina, K. Oide, H. Sakai, S. Sakanaka,
M. Shimada, K. Tsuchiya, K. Umemori, M. Yamamoto,
S. Chen, T. Konomi, T. Kubo



(JAEA) R. Hajima, N. Nishimori

The design study has been done under collaboration with a Japanese company.

Outline

- Introduction
- Injector Design
- Main Linac Design
- Bunch Compression & Decompression Scheme
- Design of Arc & Chicane
- Bunch Compression Simulation
- FEL Performance
- Summary and Outlook

Motivation

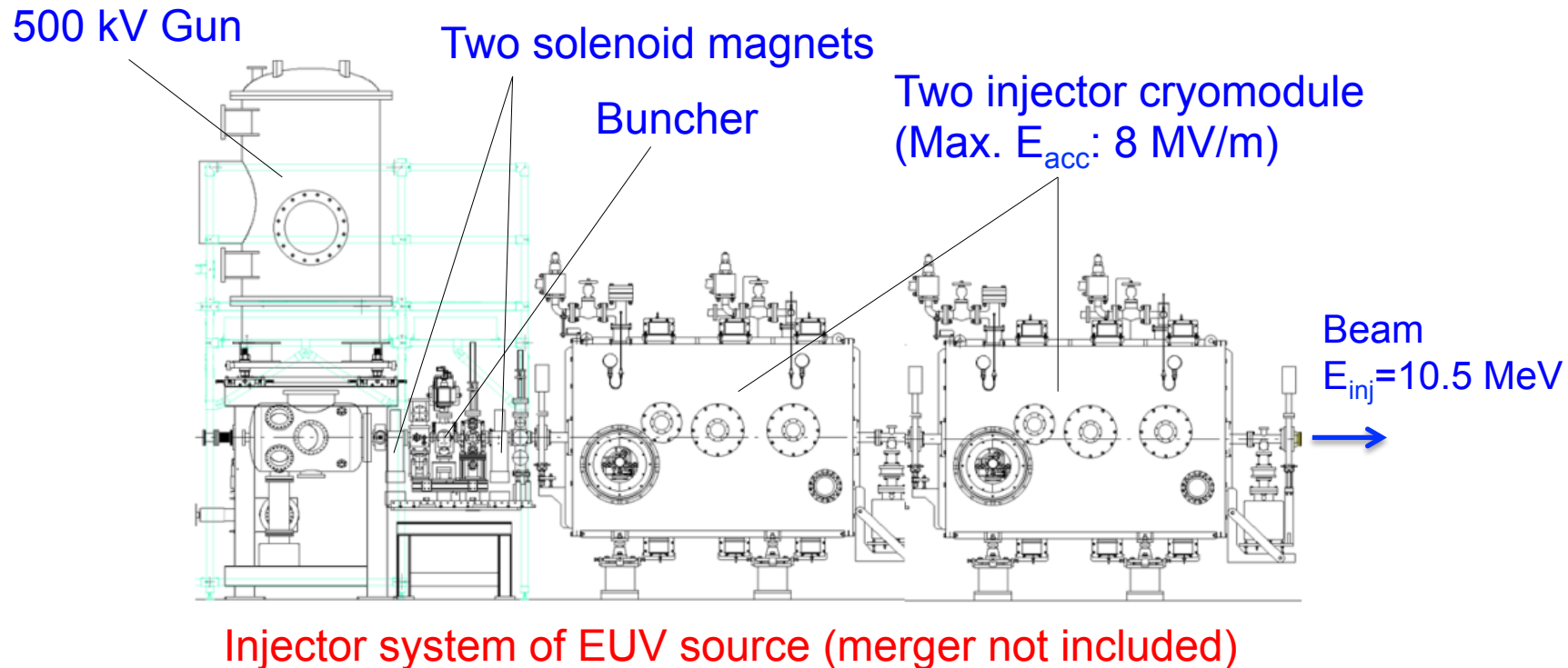
- 10-kW class EUV sources are required in the future for lithography
- The order of EUV-FEL size and cost can be acceptable
- ERL-FELs have merits of energy recovery, low dumped beam power and activation

Design Concept

- Target : 10kW power @ 13.5 nm, 800 MeV
- Use available technology without too much development
- Make the most of the cERL designs, technologies and operational experiences

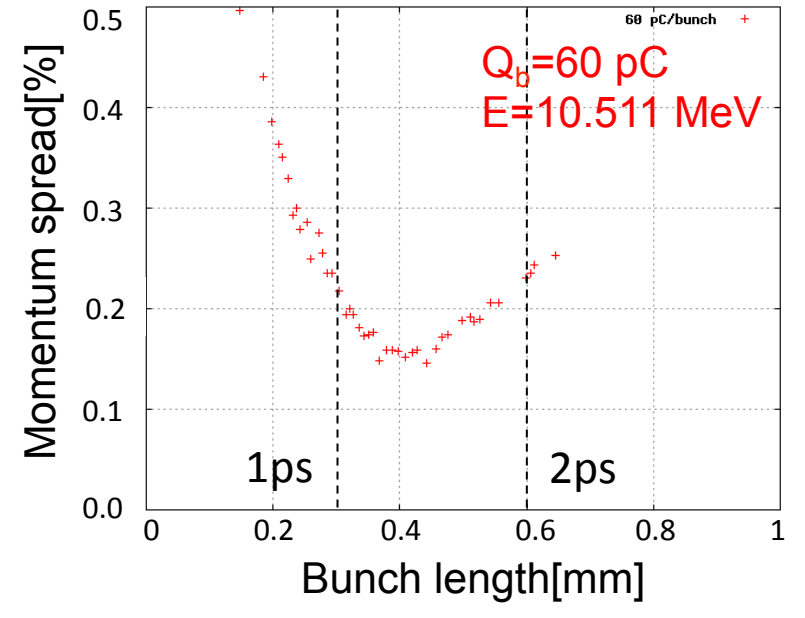
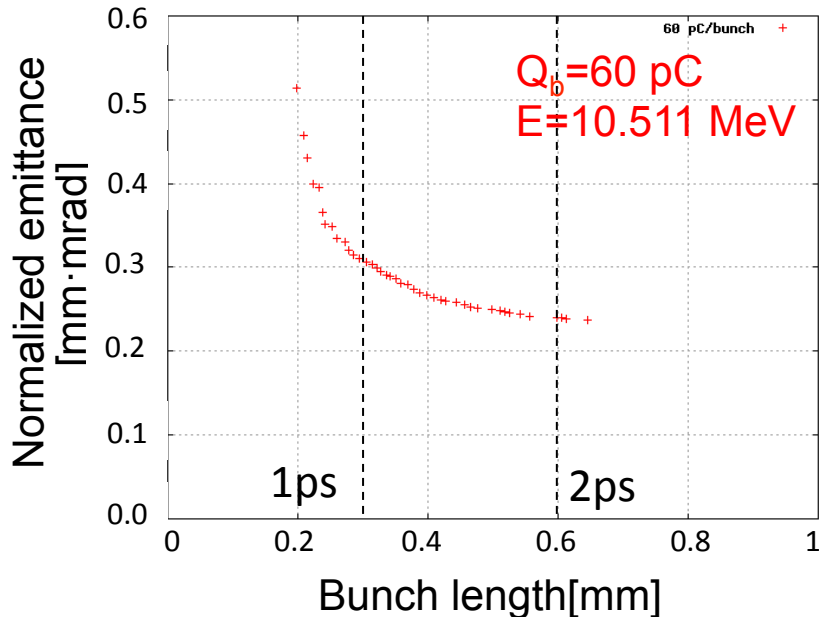
Injector Design

- DC Photocathode gun with the same structure of 2nd gun at cERL
- Two cERL cryomodules with six 2-cell SC cavities for $E_{inj}=10.5$ MeV
- Two solenoid magnets and one buncher cavity
- New merger (under design)



Injector Parameters

Optimization of injector parameters before merger



Tracking by GPT

60pC/bunch

1 ps : 0.30 mm mrad, 0.25 % $\rightarrow \varepsilon_n = 0.60 \text{ mm}\cdot\text{mrad}$, $\sigma_p/p = 0.25 \%$ @ merger exit

2 ps : 0.25 mm mrad, 0.25 % $\rightarrow \varepsilon_n = 0.55 \text{ mm}\cdot\text{mrad}$, $\sigma_p/p = 0.25 \%$ @ merger exit

100pC/bunch

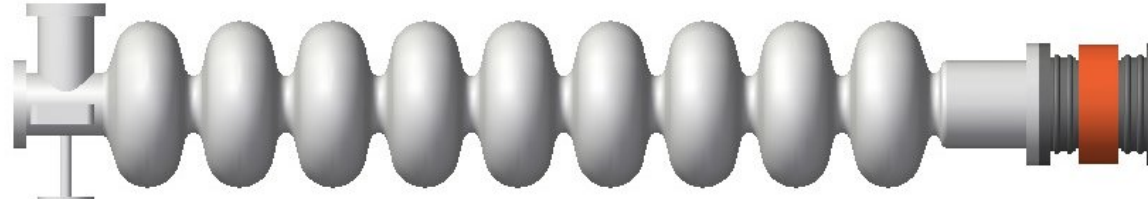
1 ps : 0.57 mm mrad, 0.35 % $\rightarrow \varepsilon_n = 0.80 \text{ mm}\cdot\text{mrad}$, $\sigma_p/p = 0.35 \%$ @ merger exit

2 ps : 0.35 mm mrad, 0.16 % $\rightarrow \varepsilon_n = 0.60 \text{ mm}\cdot\text{mrad}$, $\sigma_p/p = 0.16 \%$ @ merger exit

The results are used as initial values for simulations including bunch compression.

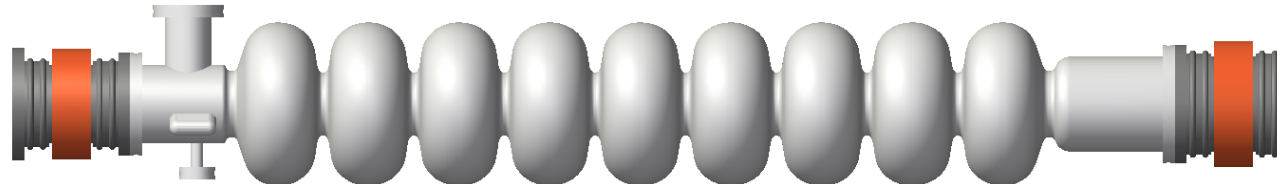
Design of Main Linac Cavity

ERL-EUV cavity (Model 1) – TESLA-type 9-cell cavity + 108 ϕ beam pipe



Under design. A large-aperture beam pipe will be also applied to the left side.

cERL cavity (Model 2) – stably operated at ~8.5 MV/m

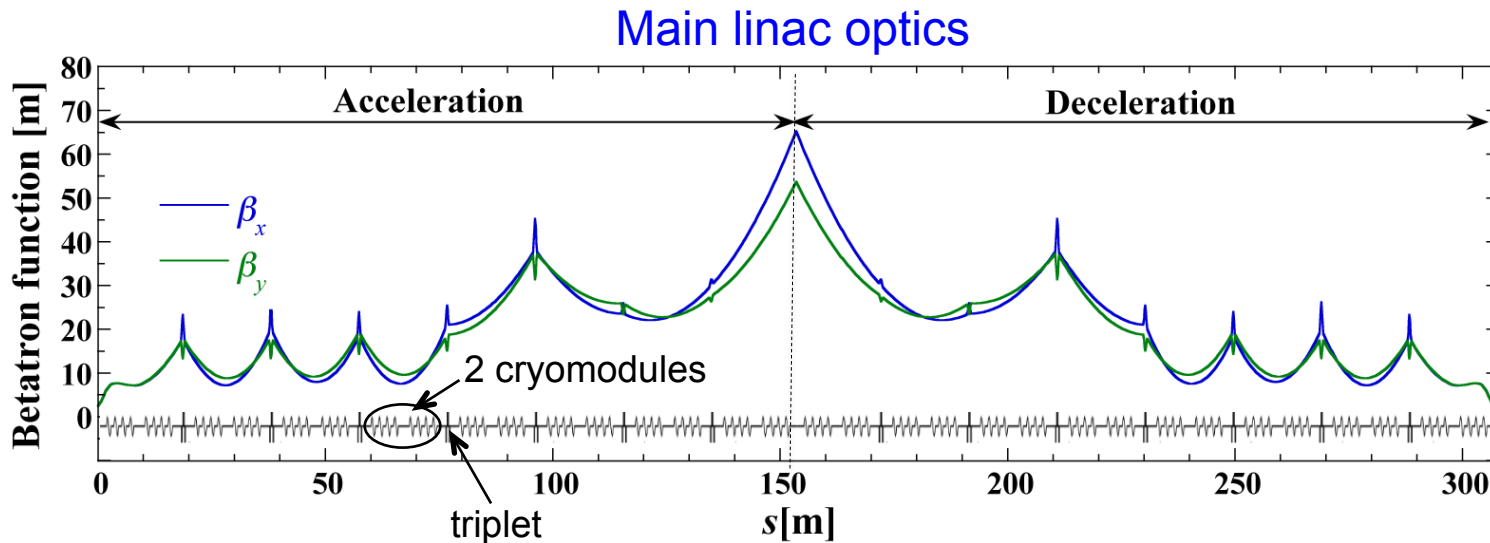


Parameters for acceleration mode

	Model 2	Model 1		Model 2	Model 1
Frequency	1300 MHz	1300 MHz	Iris diameter	80 mm	70 mm
R_{sh}/Q	897 Ω	1007 Ω	$Q_o \times R_s$	289 Ω	272 Ω
E_p/E_{acc}	3.0	2.0	H_p/E_{acc}	42.5 Oe/(MV/m)	42.0 Oe/(MV/m)

Stable operation at 12.5 MV/m seems achievable due to reduced E_p/E_{acc} .

Main Linac Optics



■ Main Linac

- 64 cavities in 16 cryomodules (4 cavities/cryomodule)
- $E_{acc} \approx 12.5$ MV/m

■ Optics

- Focusing of quadrupole triplet at every two cryomodules
- Body/edge focusing of cavities
- Betatron function optimization against BBU $\rightarrow I_{th,BBU} > 190$ mA
- Symmetric for acceleration and deceleration

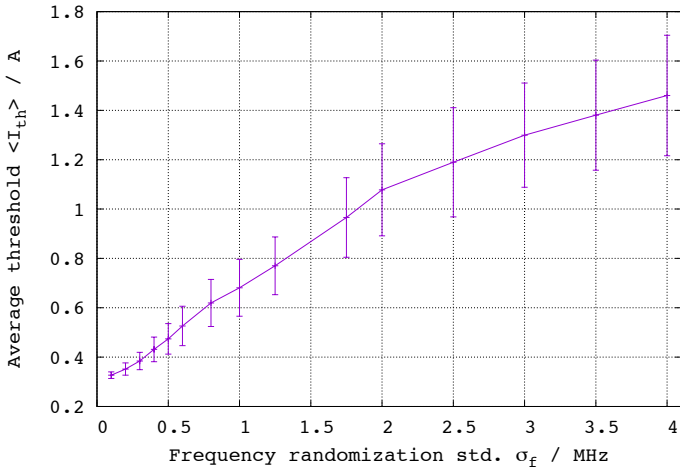
HOM BBU

HOM-BBU threshold current is calculated by Simulation code *bi*.

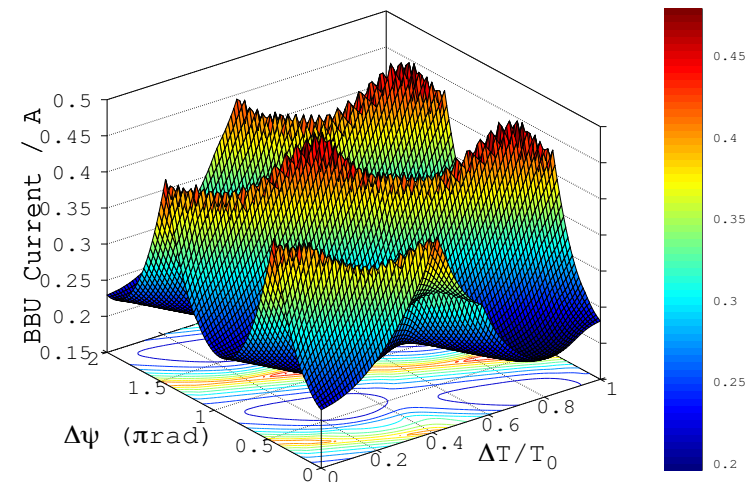
HOM parameters of Model 1 cavity

f	Q_e	R/Q	$(R/Q) Q_e/f$	ModeType
[GHz]		[Ω/cm^2]	[$\Omega/cm^2/GHz$]	
1.866	7732	6.43	26659	TM_{110} $6\pi/9$
1.874	11655	8.77	54526	TM_{110} $5\pi/9$
1.879	18360	1.95	19089	TM_{110} $4\pi/9$
2.575	4899	21.32	40557	TE_{121} $\pi/9$
3.082	33608	0.98	10676	TM_{121} $5\pi/9$

HOM randomization effects



Calculation of BBU threshold current



Scan over the betatron phase advance (0- 2π) and return loop length (in one period of the base mode). Minimum BBU current is found to be about **195 mA**. (**478mA maximum**).

Considering a Gaussian frequency distribution between linac cavities, the average BBU threshold current grows with the frequency spread σ_f increases, reaching about **1.1A** when $\sigma_f = 2\text{MHz}$.

BBU threshold current is well above the expected average current.

HOM Heating

Non-resonant heating

Parasitic loss absorbed at HOM damper

$$P_{loss} = k_{loss} Q_b^2 f_b$$

k_{loss} : Loss factor, Q_b : bunch charge
 f_b : bunch frequency

Estimation of loss factor

$k_{loss} \sim 20 \text{ V/pC} @ 1 \text{ ps}$
 $\sim 15 \text{ V/pC} @ 2 \text{ ps}$

Examples of parasitic loss power

Bunch length @cavity	9.75mA x 2 60pC 162.5MHz	8mA x 2 100pC 81.25MHz
1 ps	23.4 W	32 W
2 ps	17.6 W	24 W

Max. absorption power of HOM damper :
30 W (first target), **100 W** (final goal)

Heating resonant to monopole HOMs

Difference between monopole HOM frequency and harmonics of bunch frequency

monopole f _{HOM} [MHz]	Bunch frequency f _b [MHz]							
	325	260	162.5	135.4	130	100	81.25	
2393	207	207	118	44	53	7	45	
2427	173	173	152	10	87	27	11	
2442	158	158	158	5	102	42	5	
2447	153	153	153	10	107	47	10	
2452	148	148	148	15	112	52	15	
2453	147	147	147	16	113	53	16	
2459	141	141	141	22	119	59	22	
3848	52	208	52	57	52	48	52	
3851	49	211	49	60	49	51	49	
3852	48	212	48	61	48	52	48	
3853	47	213	47	62	47	53	47	

 : frequency difference within 10 MHz

Max. absorption power of the HOM damper restricts the bunch charge, length and frequency.
The bunch frequency should be selected so as to avoid the resonant heating.

FEL Parameters

FEL power at saturation

$$P_{sat} \approx \rho_{FEL} P_{electron}, \quad P_{electron} = EI_{av}$$

Pierce parameter

$$\rho_{FEL} = \left[\frac{1}{16} \frac{I_p}{I_A} \frac{K^2 [JJ]^2 \lambda_u^2}{\gamma^3 \sigma_x \sigma_y (2\pi)^2} \right]^{1/3}$$

$$I_p = \frac{Q_b}{\sqrt{2\pi}\sigma_t}, \quad I_A = 17kA \quad \sigma_x = \sqrt{\gamma\varepsilon_{nx}\beta_x}, \quad \sigma_y = \sqrt{\gamma\varepsilon_{ny}\beta_y}$$

$$[JJ] = J_0(\xi) - J_1(\xi), \quad \xi = K^2 / (4 + 2K^2) \quad \text{Planar undulator}$$

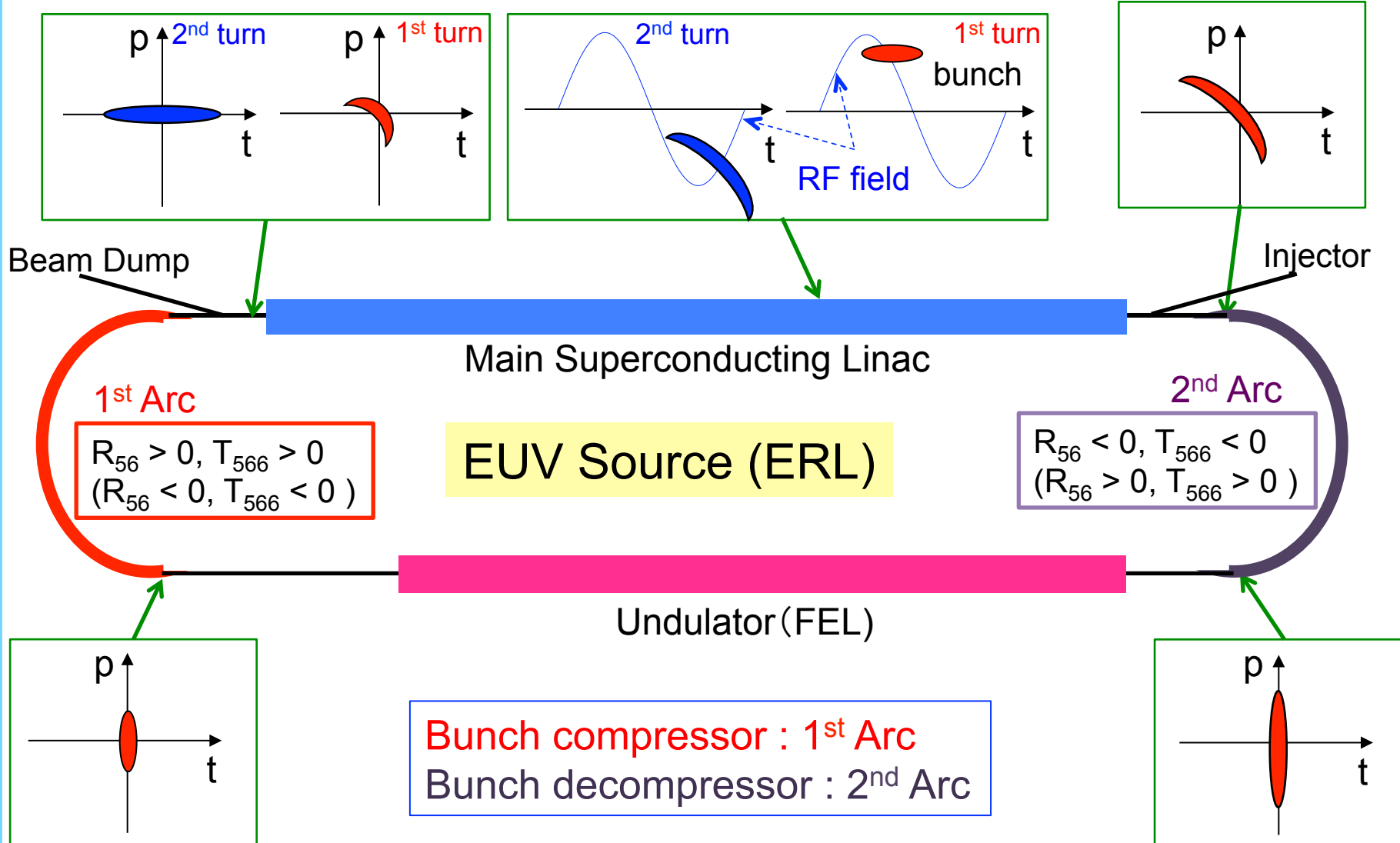
$$[JJ] = 1 \quad \text{Helical undulator}$$

Photon wavelength and undulator parameters

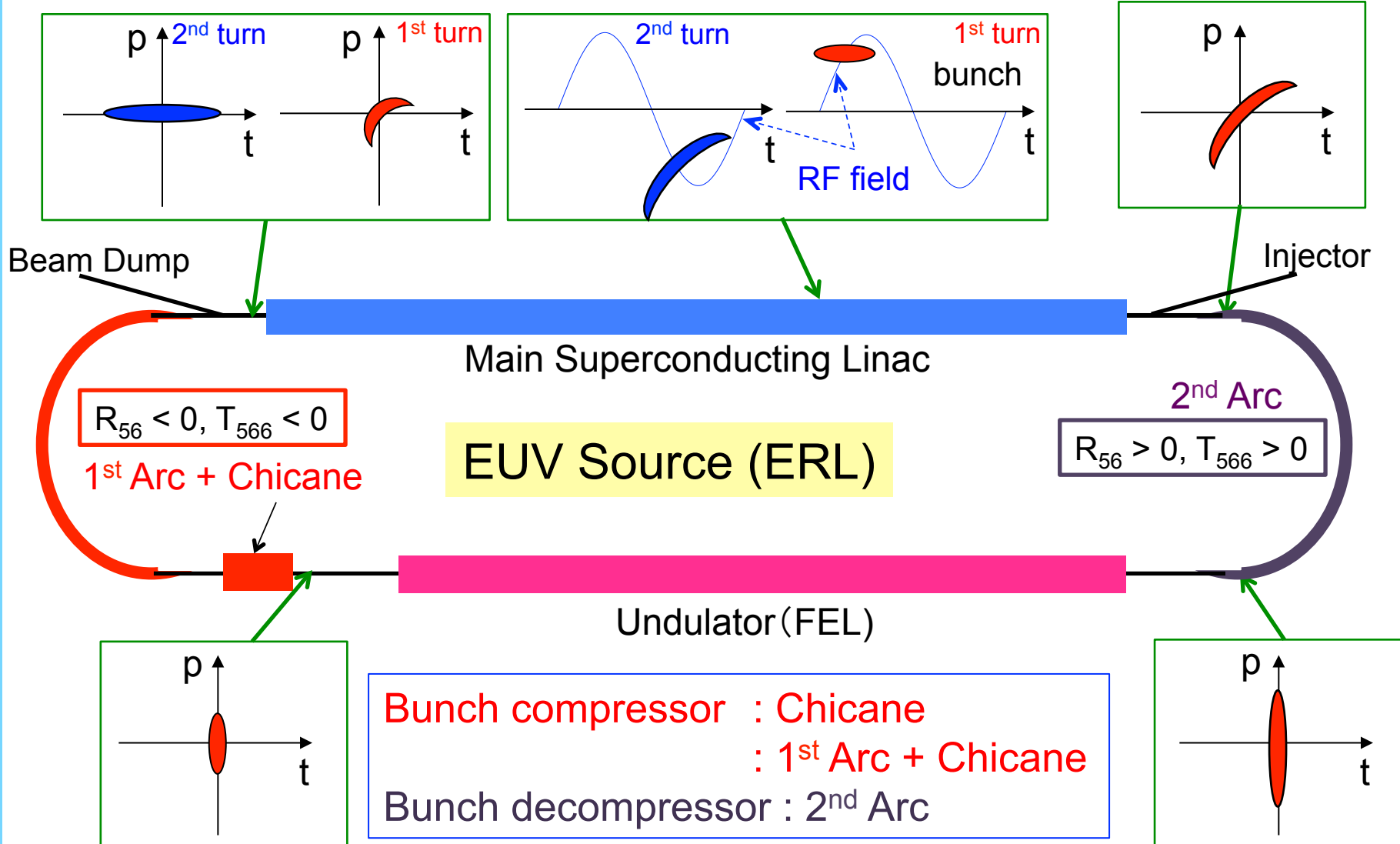
$$\lambda = \frac{\lambda_u}{2\gamma^2} \left(1 + \frac{K^2}{2} \right) \quad K = K_y \quad \text{Planar undulator}$$
$$K = \sqrt{2}K_x = \sqrt{2}K_y \quad \text{Helical undulator}$$

High peak current and low emittance are important for FEL power.

Bunch compression and decompression scheme (1)



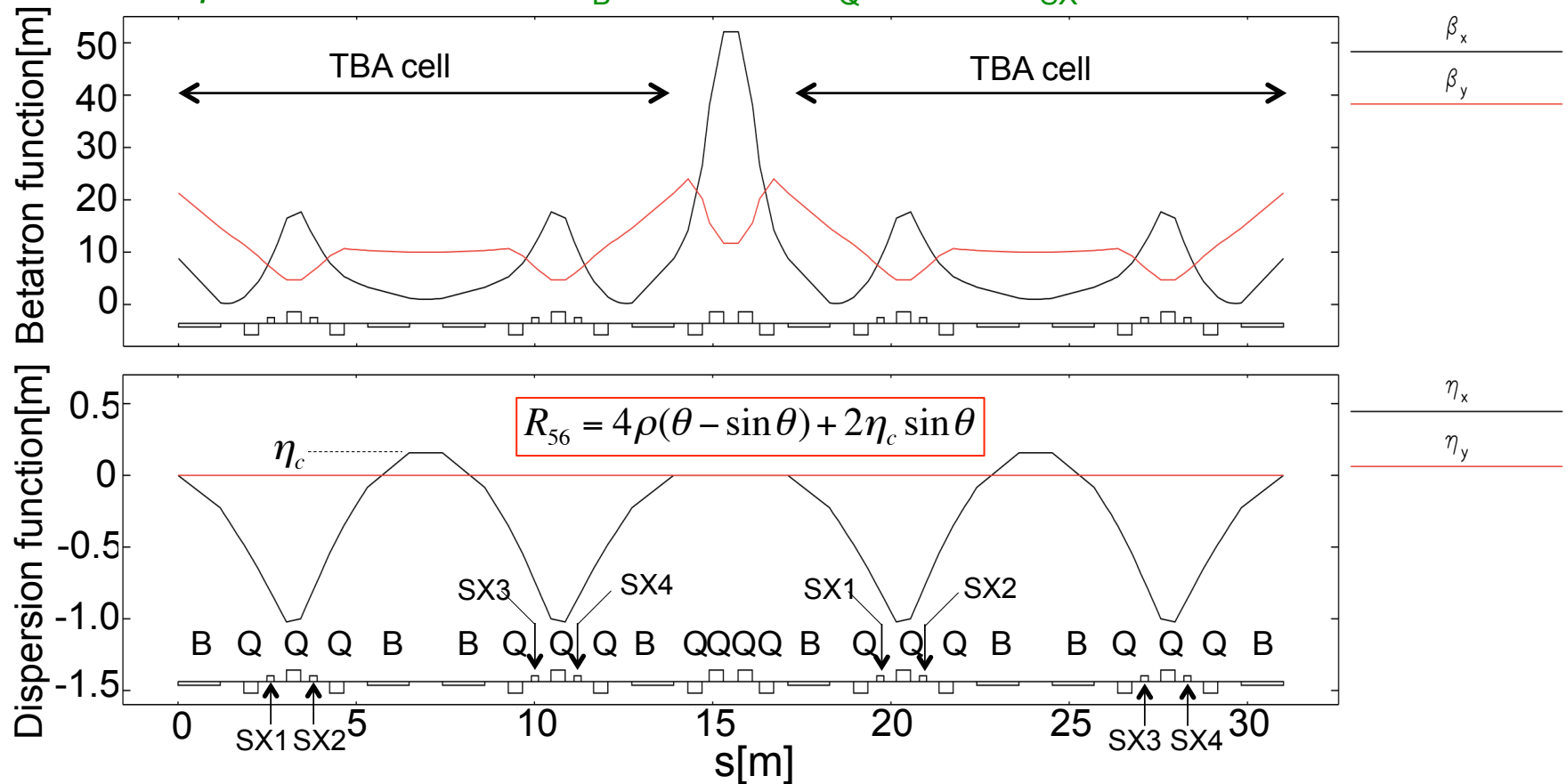
Bunch compression and decompression scheme (2)



Design of Arc Sections (1)

2-cell TBA lattice and optics ($R_{56}=0.0$ m)

$\rho=3$ m, $\theta=\pi/8$ rad, $L_B=1.178$ m, $L_Q=0.4$ m, $L_{SX}=0.2$ m

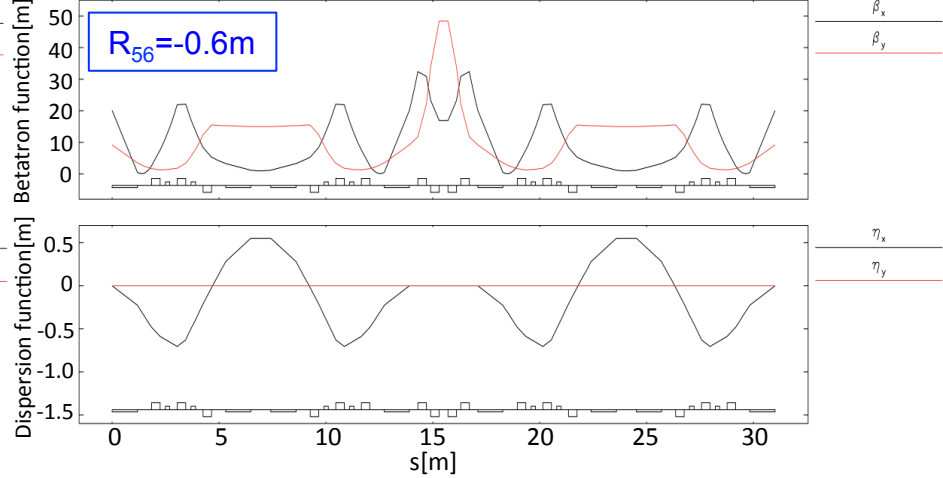
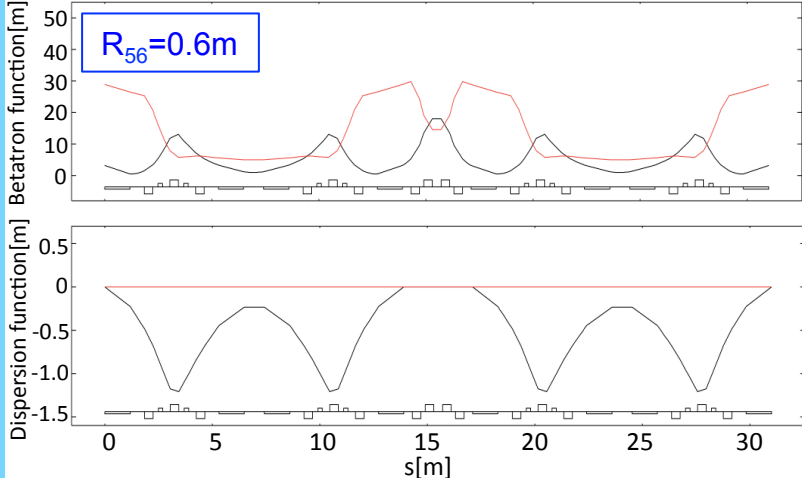
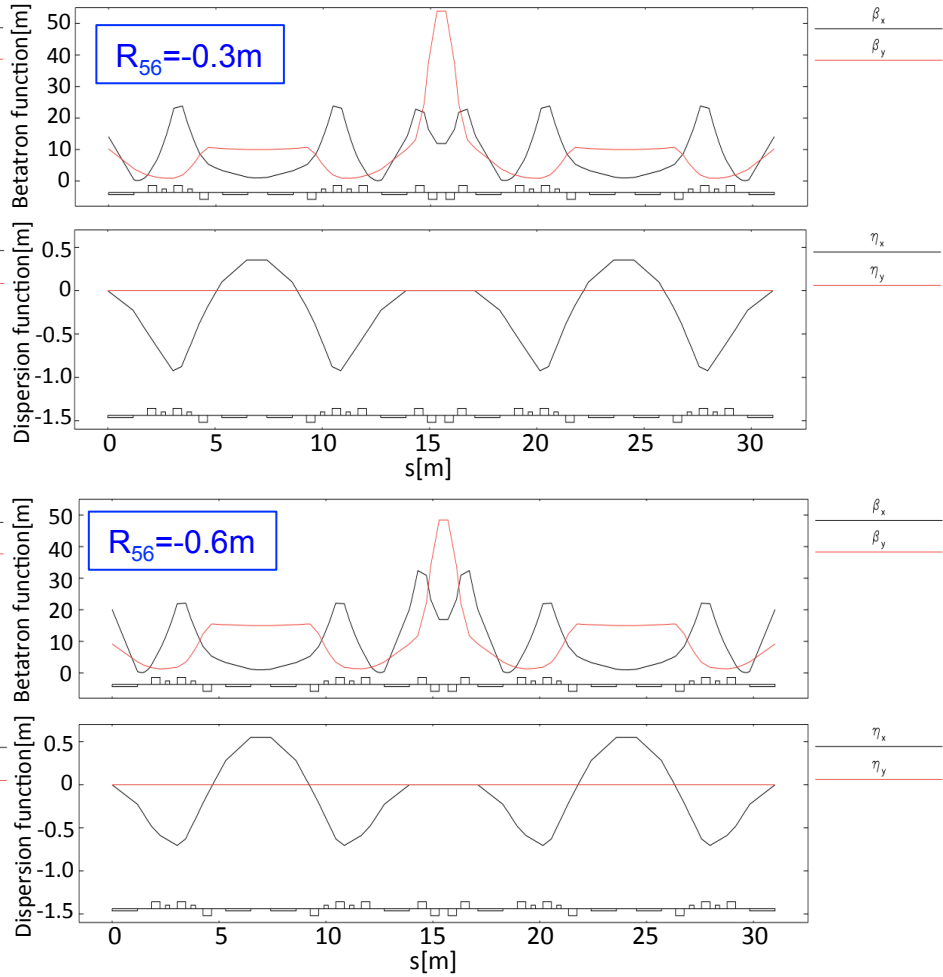
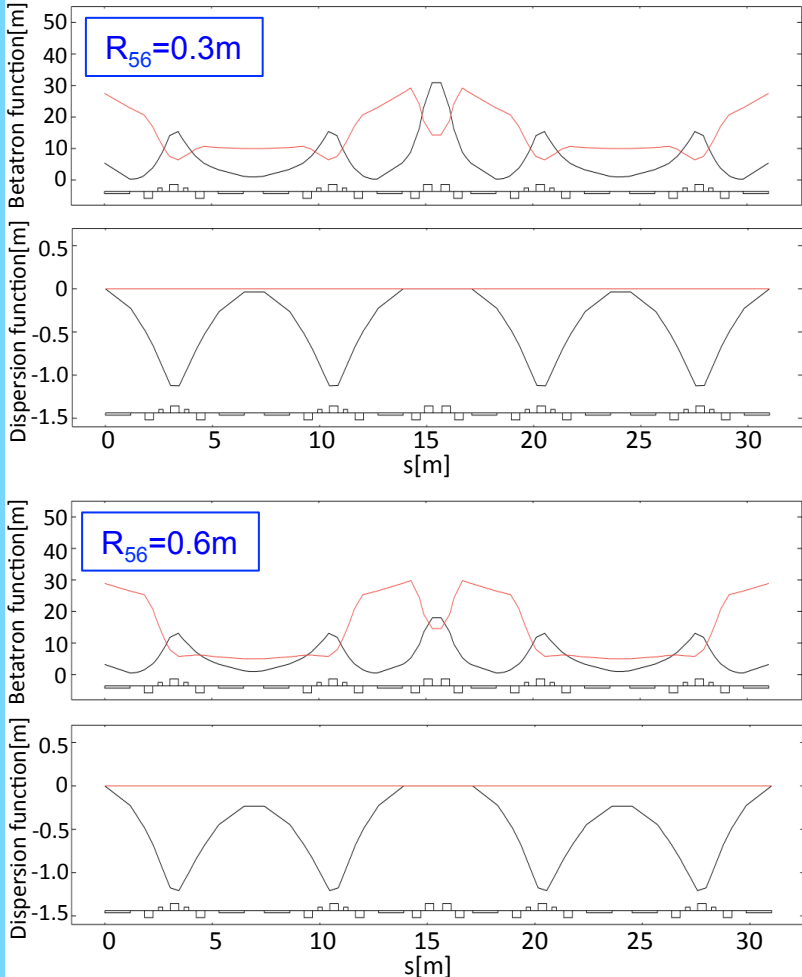


B: Bending magnet, Q: Quadrupole magnet, SX: Sextupole magnet

Eight sextupole magnets can be inserted in the arc to optimize T_{566} .

Design of Arc Sections (2)

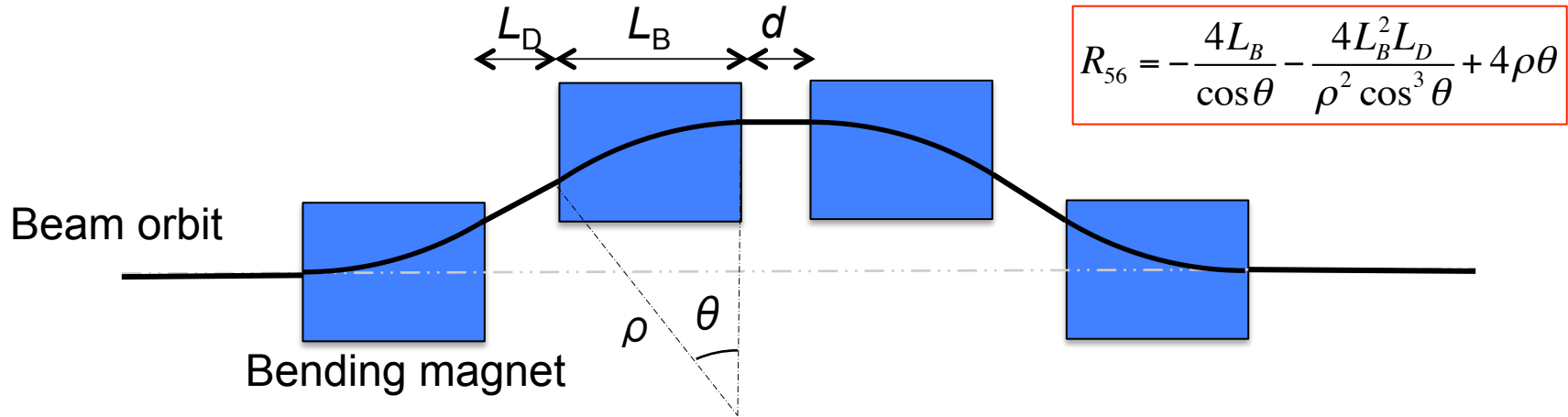
Examples of 2-cell TBA optics with different R_{56}



The 2-cell TBA lattice has a wide dynamic range of R_{56} .
Momentum acceptance is more than 4% for horizontal half-aperture of $\sim 5\text{cm}$.

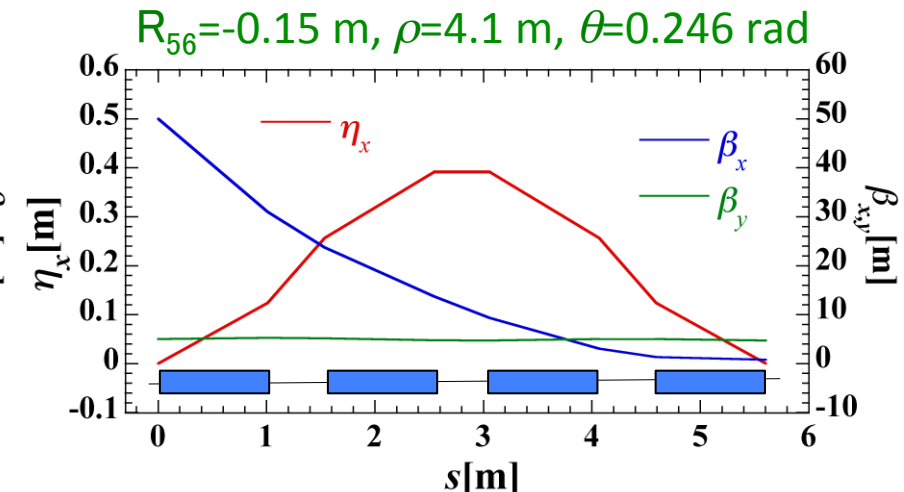
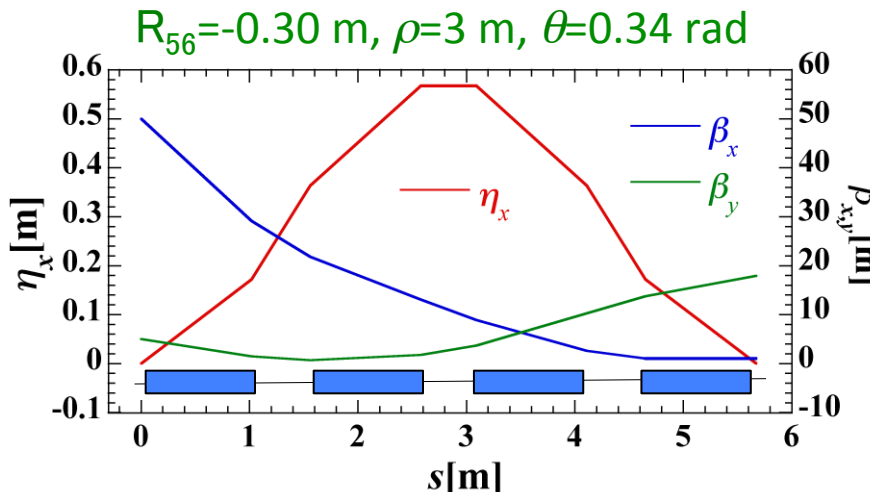
Design of Chicane

Four-magnet chicane

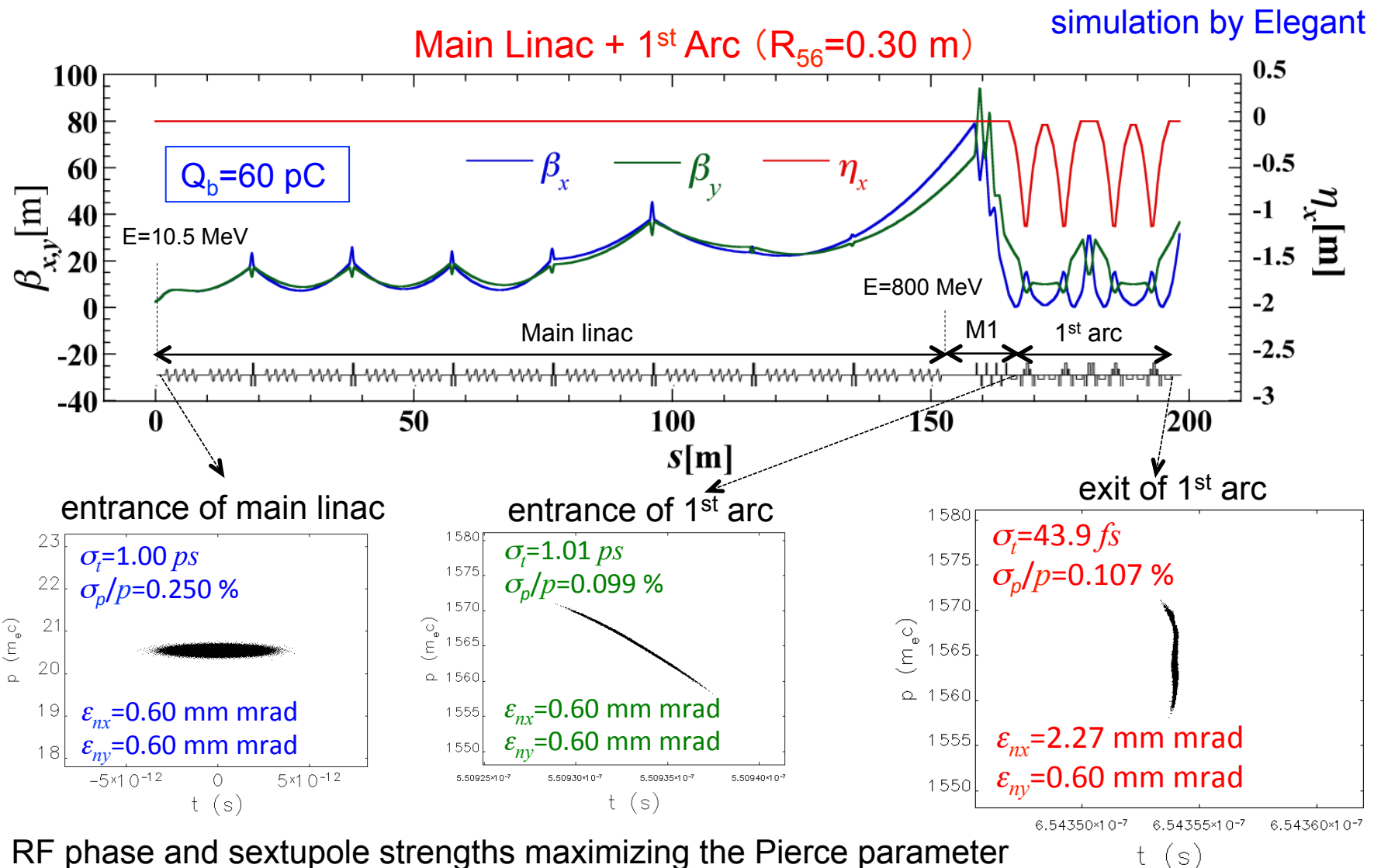


$$R_{56} = -\frac{4L_B}{\cos\theta} - \frac{4L_B^2 L_D}{\rho^2 \cos^3\theta} + 4\rho\theta$$

Chicane optics for $L_B=1\text{m}$ and $L_D=d=0.51\text{m}$



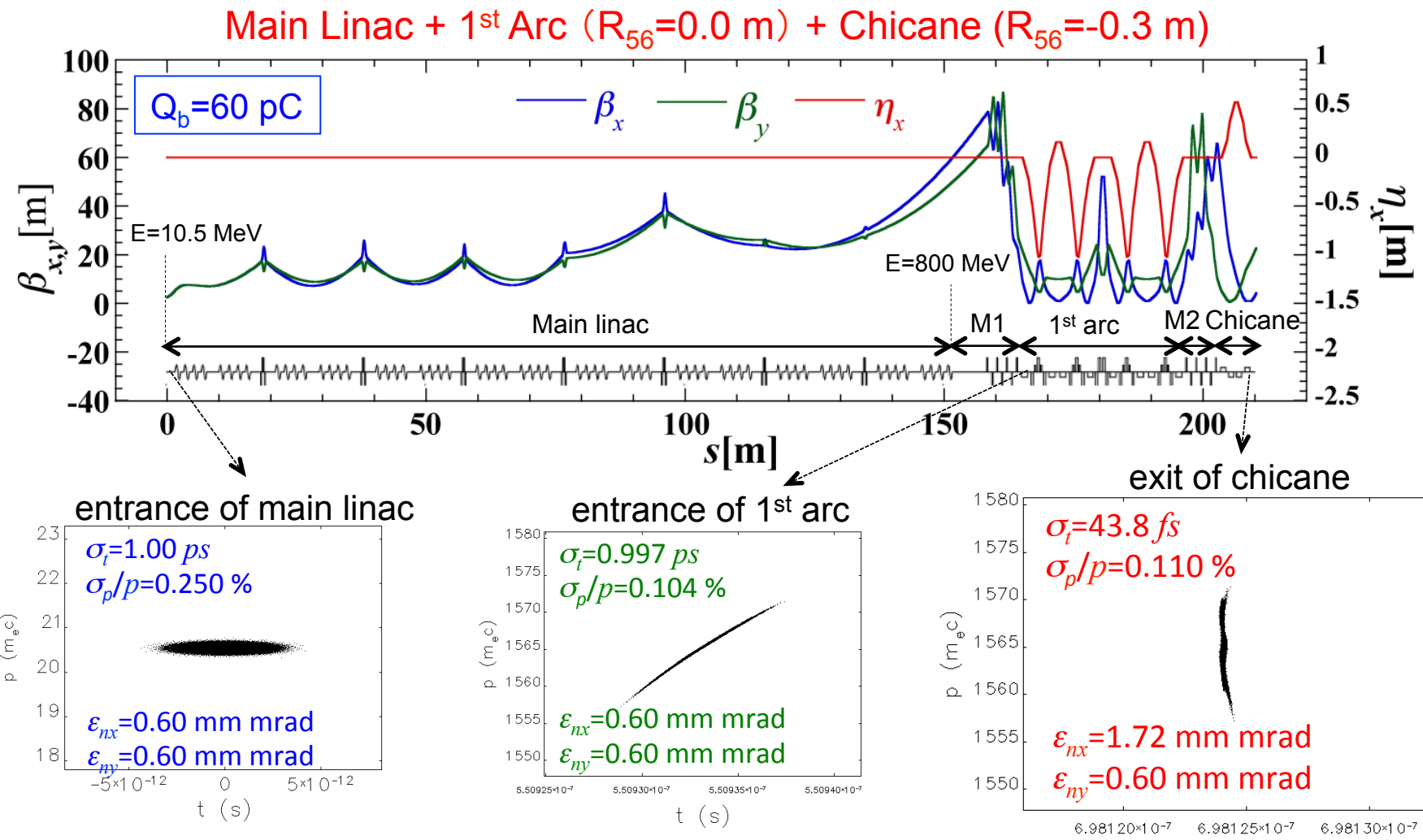
Bunch Compression by Arc



RF phase and sextupole strengths maximizing the Pierce parameter

$$K_2(\text{SX1}) = -54.6 \text{ [m}^{-3}\text{]}, K_2(\text{SX4}) = 26.4 \text{ [m}^{-3}\text{]}, \phi_{RF} = 96.7 \text{ [deg]}$$

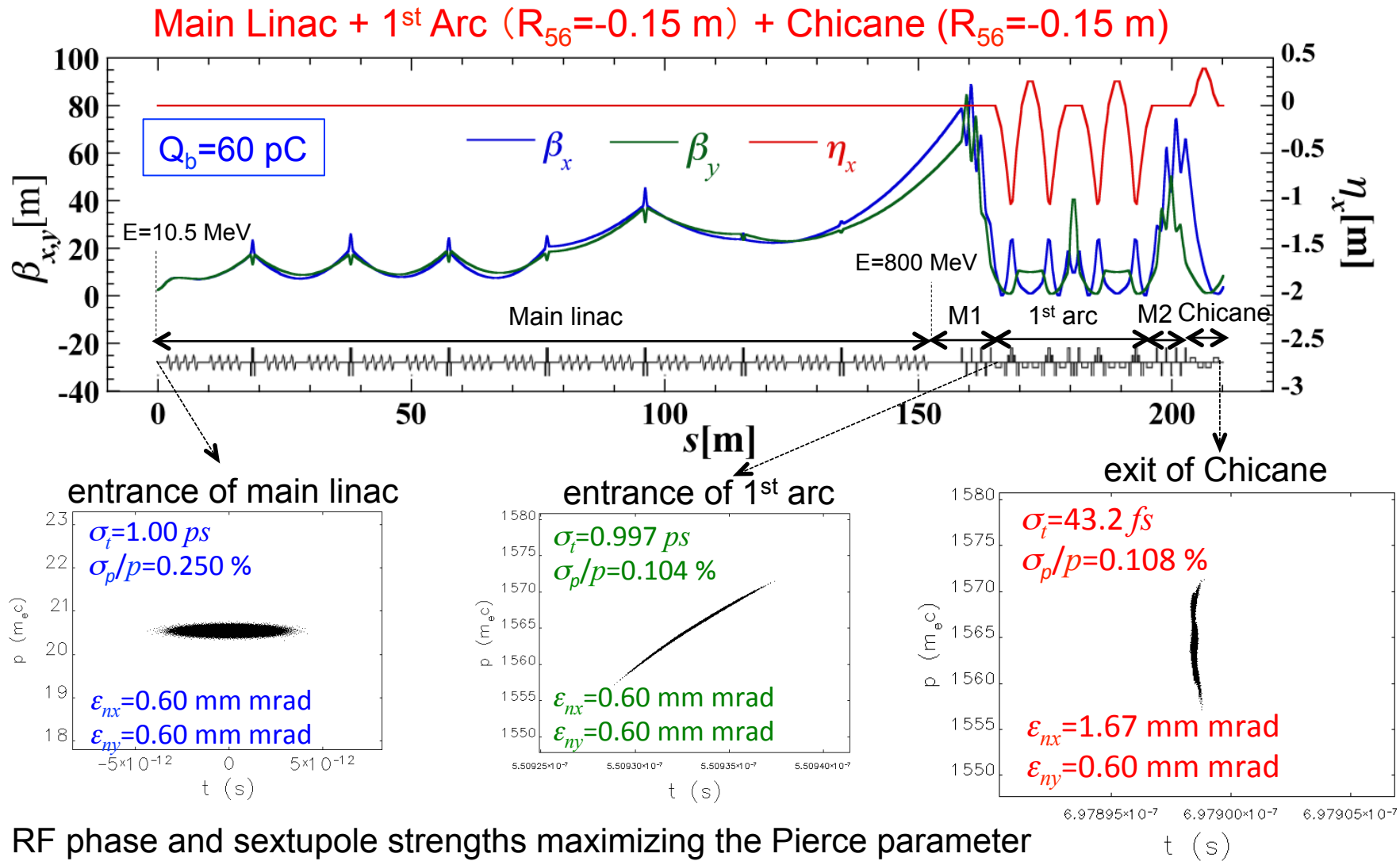
Bunch Compression by Chicane



RF phase and sextupole strengths maximizing the Pierce parameter

$$K_2(\text{SX1}) = -91.2 \text{ [m}^{-3}\text{]}, K_2(\text{SX4}) = 23.6 \text{ [m}^{-3}\text{]}, \phi_{RF} = 82.4 \text{ [deg]}$$

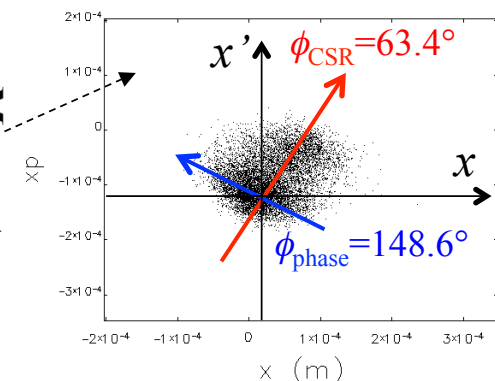
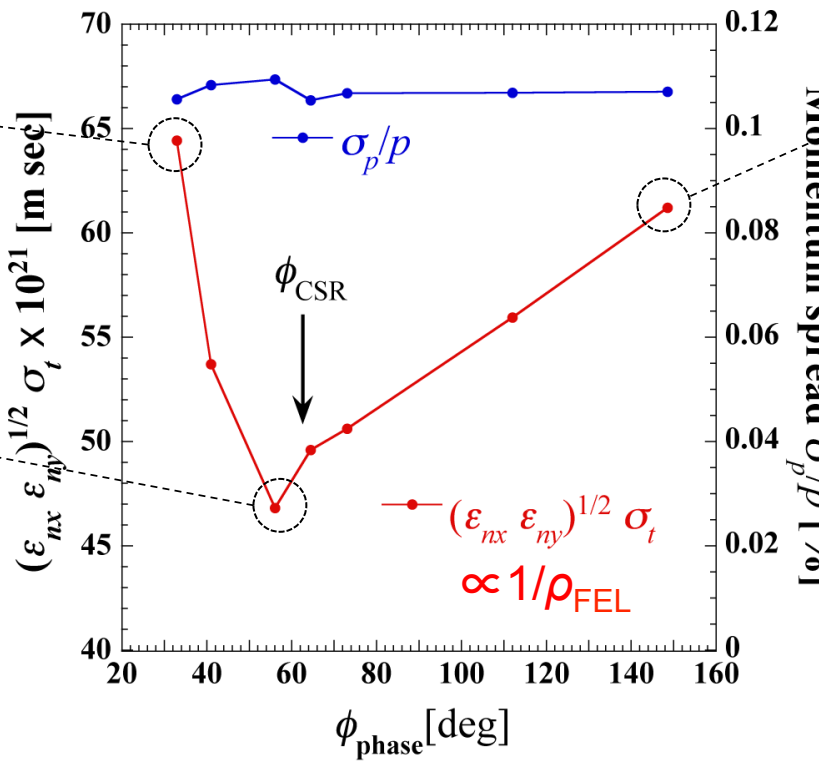
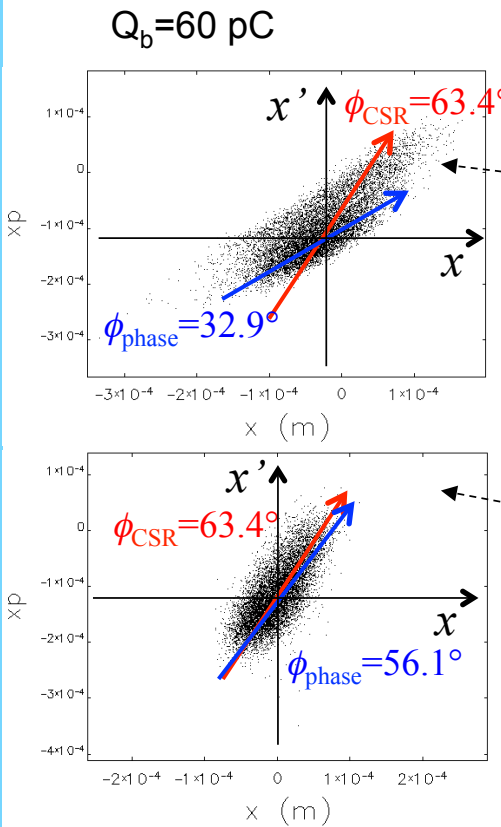
Bunch Compression by Arc & Chicane



Compensation of CSR effects (1)

Minimization of CSR-induced horizontal emittance growth

Phase ellipse angle vs beam/FEL parameters at chicane exit
(bunch compression by chicane)



$$\tan \phi_{CSR} = \frac{2 \tan(\theta/2)}{\rho(1 - \cos \theta)}$$

(rectangular magnet)

$$\tan 2\phi_{phase} = \frac{2\alpha_x}{\gamma_x - \beta_x}$$

The phase ellipse and CSR kick directions can be matched at chicane exit.
Such optics adjustment is difficult for bunch compression by arc.

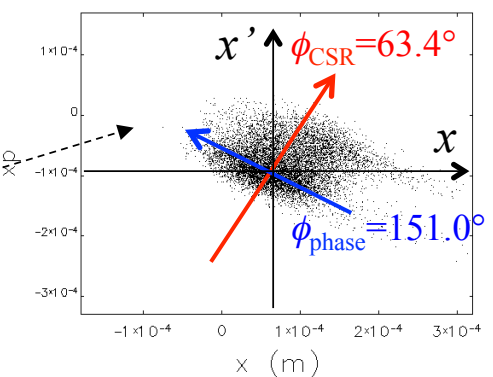
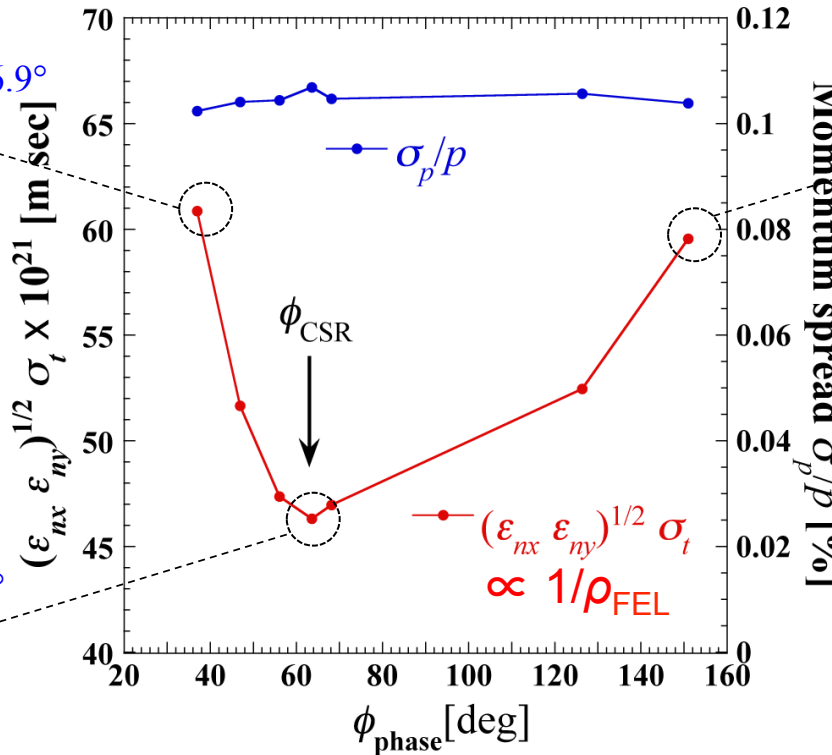
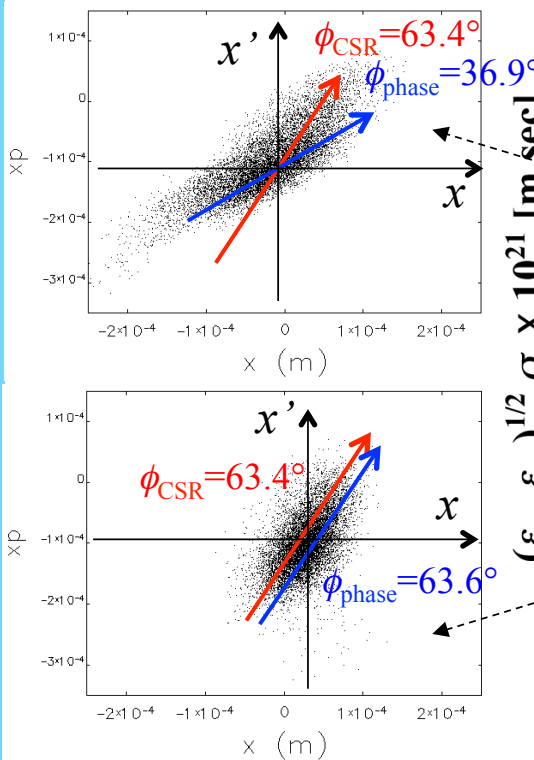
Compensation of CSR effects (2)

Minimization of CSR-induced horizontal emittance growth

Phase ellipse angle vs beam/FEL parameters at chicane exit

$Q_b = 60 \text{ pC}$

(bunch compression by arc & chicane)



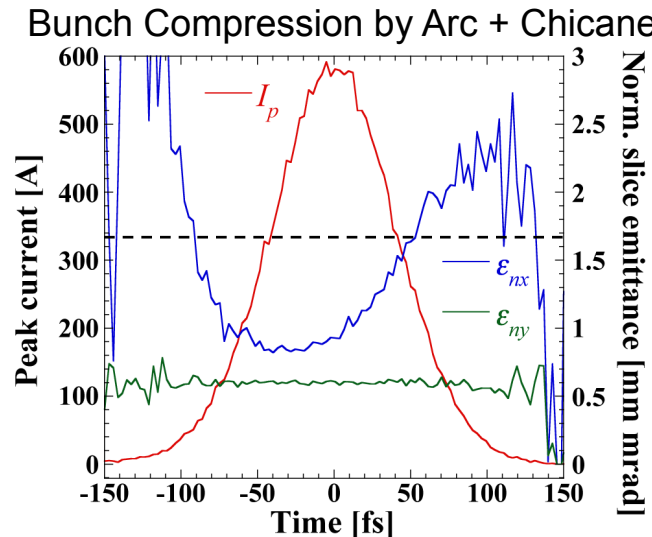
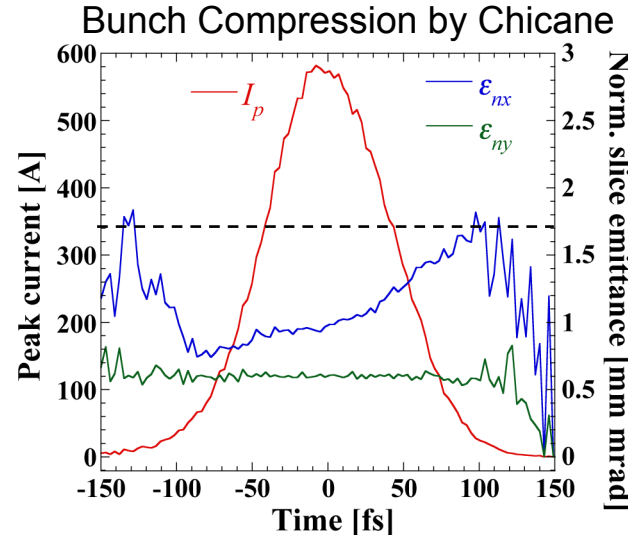
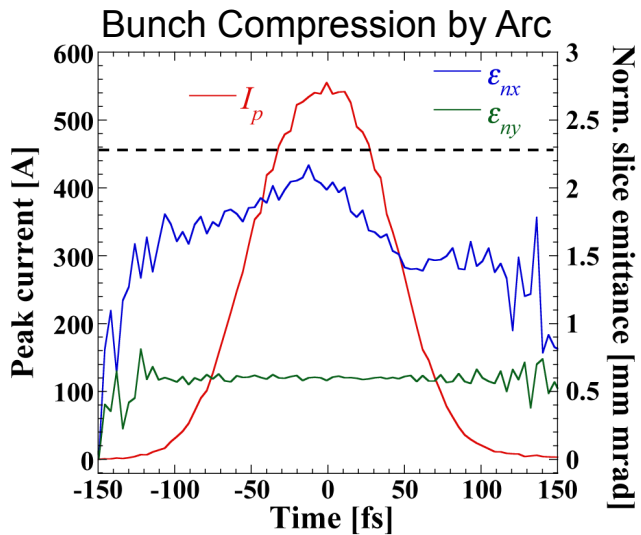
$$\tan \phi_{CSR} = \frac{2 \tan(\theta/2)}{\rho(1 - \cos \theta)}$$

(rectangular magnet)

$$\tan 2\phi_{phase} = \frac{2\alpha_x}{\gamma_x - \beta_x}$$

The phase ellipse and CSR kick directions can be matched at chicane exit.
Such optics adjustment is difficult for bunch compression by arc.

Peak Current & Slice Emittance



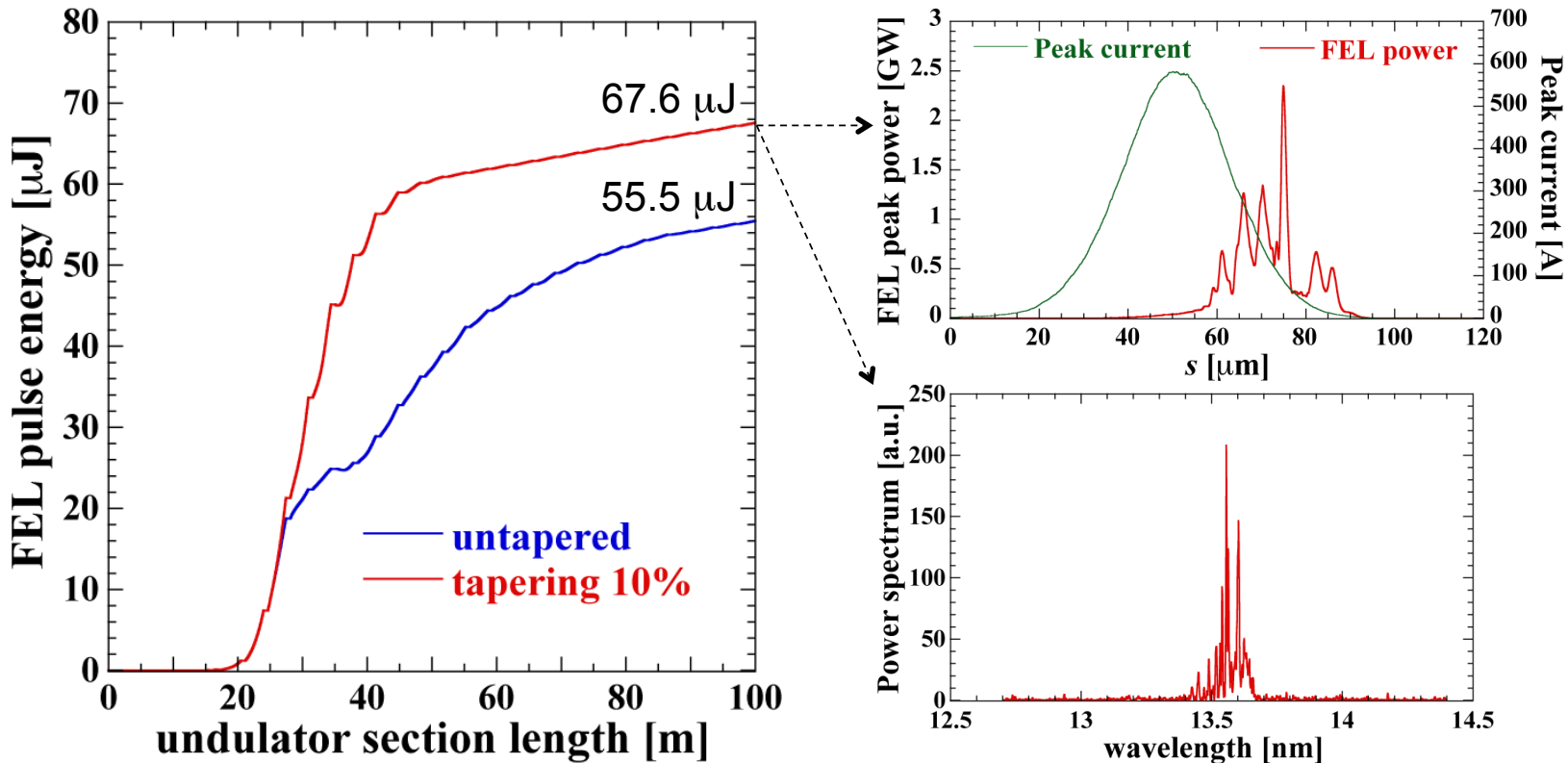
$Q_b = 60 \text{ pC}$

projected normalized
horizontal emittance

Slice emittance at high peak currents is lower than the projected emittance.

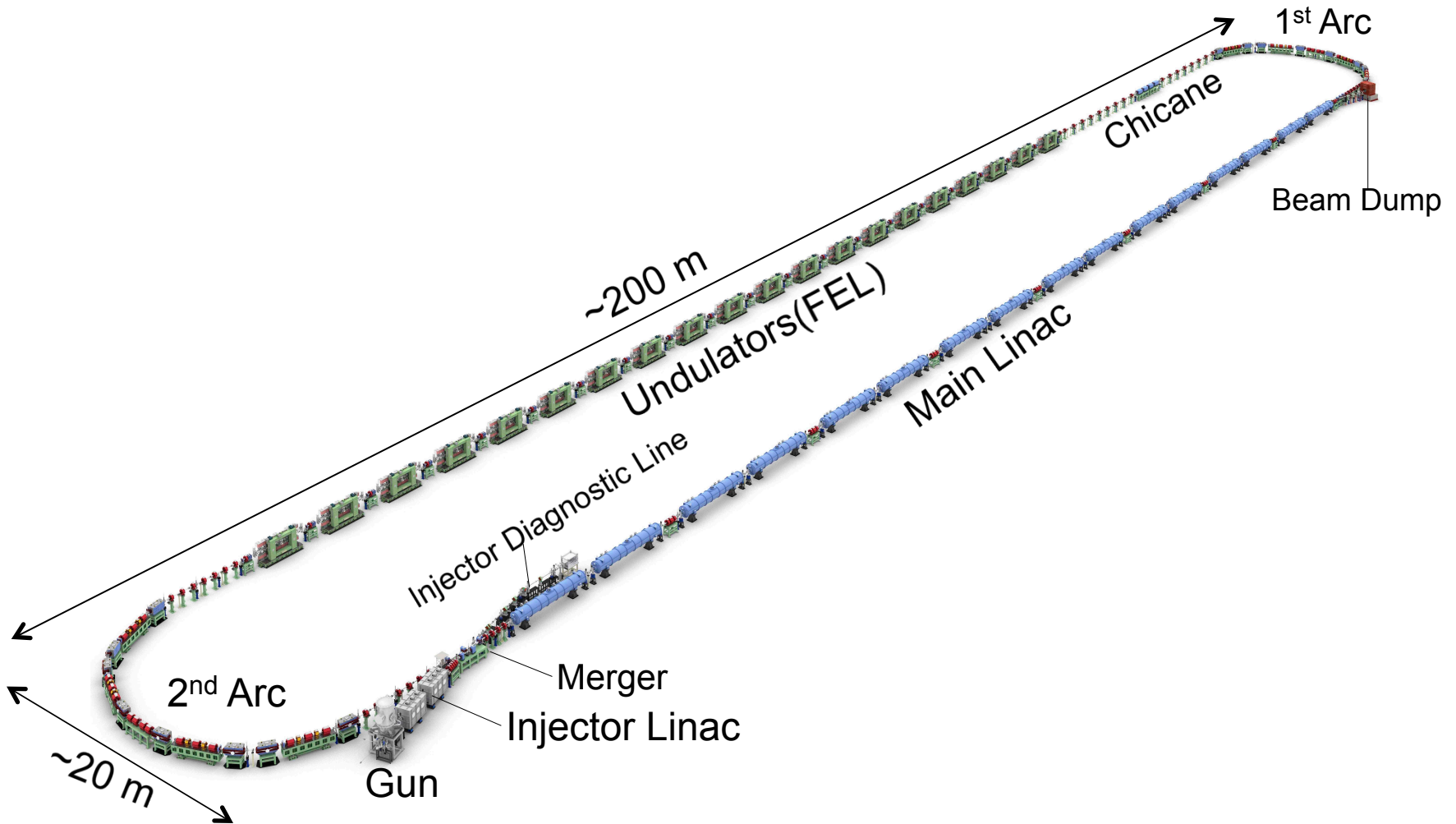
FEL Performance

Electron beam parameters: $E=800$ MeV, $Q_b=60$ pC, $f_b=162.5/325$ MHz
Helical undulator parameters: $K=1.652$, $\lambda_u=28$ mm, $L_u=2.8$ m (x 40)
Bunch compression scheme: 1st Arc + Chicane



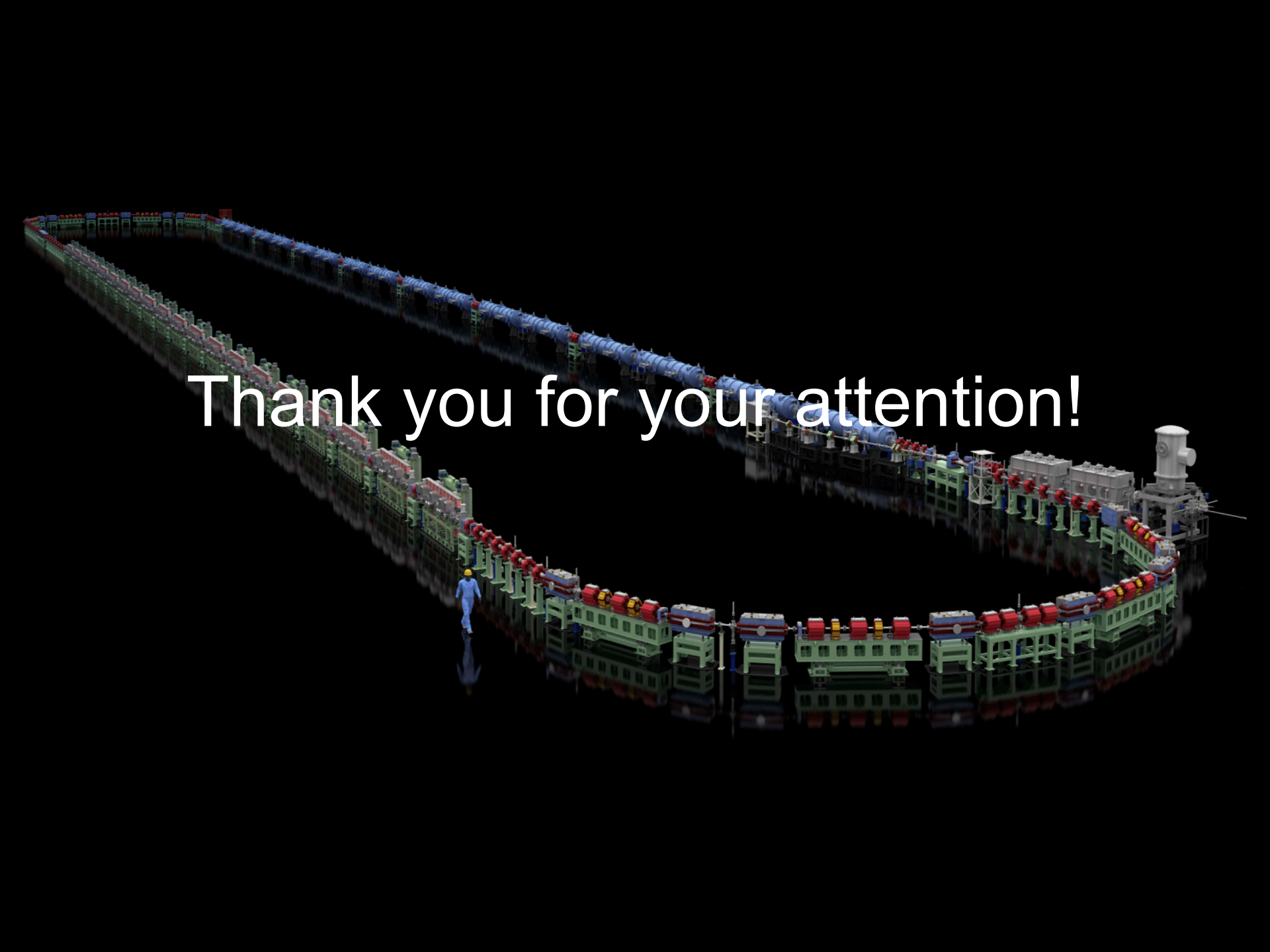
FEL power without tapering: 9.0/18.0 kW @ 9.75/19.5 mA
FEL power with 10% tapering: 11.0/22.0 kW @ 9.75/19.5 mA

Image of ERL-EUV Design



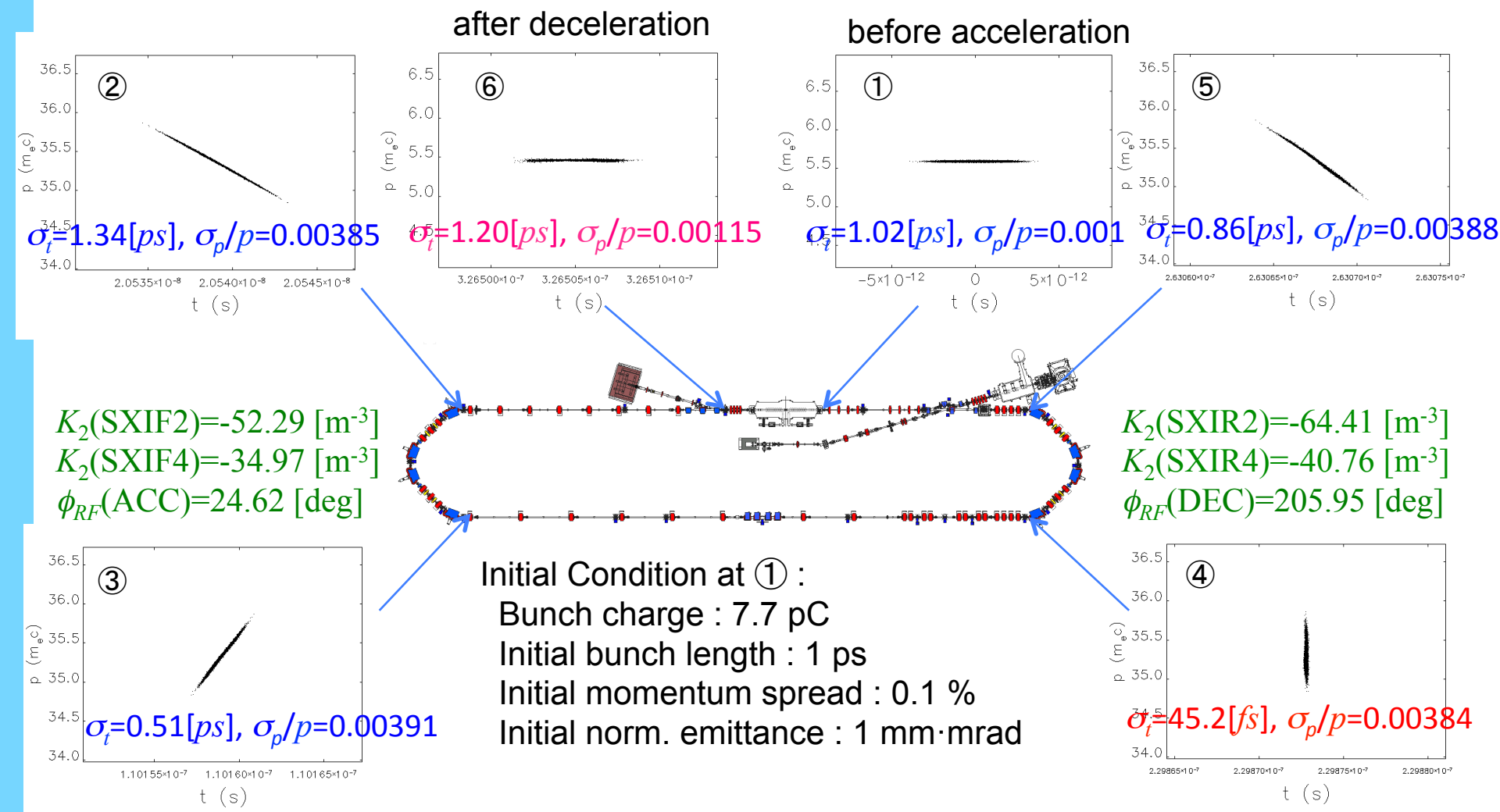
Summary & Outlook

- Design of ERL-EUV
 - Injector (gun, SRF cryomodule, tracking)
 - Main linac (cavity, optics, HOM BBU and heating)
 - Arcs and chicane (lattice, optics)
 - Bunch compression simulation
- Performance of the designed ERL-EUV
 - 9 kW power at 9.75 mA without tapering
 - 11 kW at 9.75 mA with tapering
- Further design work and optimization
 - Improvement of FEL power
(tapering, optics, beam&undulator parameters etc.)
 - Bunch decompression simulation → S2E simulation

A 3D rendering of a large particle accelerator ring, likely a synchrotron, set against a black background. The ring consists of a series of green rectangular structures connected by blue curved pipes. A small figure of a worker in a blue suit and yellow hard hat stands near the bottom left of the ring, providing a sense of scale. The ring is highly reflective, creating a clear mirror image below it.

Thank you for your attention!

Bunch Compression and Decompression at cERL



Bunch compression and decompression are successfully simulated at cERL.